NO by bimolecular reaction. Furthermore, as time passes, the expansion proceeds further and the sampling takes place deeper into the laser-heated region. Thus, if secondary reactions were responsible for the observed NO, then the proportion of NO should increase with increasing time. As described in the Results section, such an increase is definitely not observed under the conditions of Figures 3-5. However, if the DMNA reservoir temperature is raised 30 °C and the laser heating is increased so that $\sim 60\%$ of the DMNA is decomposed, then the partial pressures of initially produced NO_2 and dimethylamino radicals increase by an order of magnitude each, and the rate of bimolecular production of NO increases by 2 orders of magnitude. Under these conditions, we are able to see the NO_2 signal decrease, the NO signal grow substantially during the observation time, and also a growth in m/z 74 (Figure 6) for dimethylnitrosamine.

Because of the desire to have a true real-time measure of the NO_2/NO ratios, we are currently exploring the use of laser-induced fluorescence (LIF) to monitor both of these species. This is, in principle, more direct but must deal with possible ambiguities resulting from photochemical generation of NO from NO_2, photochemical generation of NO and NO_2 from DMNA itself, unknown spectroscopy of radical products, and, at large extents of reaction, with chemiluminescence from secondary reactions.

Conclusions

The observation of substantial amounts of NO, together with the ion fragments of the dimethylnitroxyl radical, on the same time scale as NO_2 is produced, and much too rapidly for significant secondary bimolecular reaction, necessitates the conclusion that this rapidly produced NO arises from an intramolecular nitro-nitrite rearrangement, followed by extremely rapid unimolecular scission of the very weak O-NO bond. Although this is analogous to similar rearrangements that have been reported for nitroalkanes[13] and nitroaromatics,[14,15] it is in contrast with previous reports that dimethylnitramine decomposition proceeds entirely by $N-NO_2$ bond scission.[1-4] At this point, we presume that this reaction proceeds, as those in the $C-NO_2$ cases appear to, as a very "loose" rearrangement with rotation of the NO_2 not being substantial until there is considerable lengthening of the $N-NO_2$ bond. The nature of this rearrangement is now being explored in this laboratory (for unsubstituted nitramine) using multiconfiguration ab initio calculations.

Acknowledgment. We acknowledge the support of the U.S. Army Research Office under Contract No. DAAC03-86-K-003 and the U.S. Air Force Office of Scientific Research under Contract No. F496220-85-K-00006. The Chemical Physics Laboratory computer system (VAX 11/750) was purchased under NSF Grant PHY-8114611.

Registry No. DMNA, 4164-28-7.

---

(13) Wodtke, A. M.; Hintsa, E. J.; Lee, Y. T. *J. Phys. Chem.* **1986**, *90*, 3549.

(14) Gonzalez, A. C.; Larson, C. W.; McMillen, D. F.; Golden, D. M. *J. Phys. Chem.* **1985**, *89*, 4809.

(15) Tsang, W.; Robaugh, D.; Mallar, W. G. *J. Phys. Chem.* **1986**, *90*, 5968.

Rates, Products, and Mechanisms in the Gas-Phase Hydrogenolysis of Phenol between 922 and 1175 K

Jeffrey A. Manion and Robert Louw*

Center for Chemistry and the Environment, CCE, Gorlaeus Laboratories, Leiden University, P.O. Box 9502, Leiden, The Netherlands *(Received: May 11, 1988; In Final Form: October 4, 1988)*

The thermolysis of 0.6-6 vol % phenol in H_2 at atmospheric pressure has been examined between 922 and 1175 K. Two major initial overall reactions were observed, yielding benzene and CO, respectively: $C_6H_5OH + H_2 \rightarrow C_6H_6 + H_2O$ (3) and $C_6H_5OH \rightarrow C_5H_6 + CO$ (4). Secondary products include methane, acetylene, ethylene, ethane, naphthalene, indene, and small amounts of other hydrocarbons; these products appear to stem mainly from the C_5 species(s) formed in the course of reaction 4. Dibenzofuran was the only observed oxygen-containing product, and for a 6% phenol feed, ≤ 0.06 mol % was formed. Dibenzo-*p*-dioxin, if formed, was below our detection limit of ca. 50 ppm. Benzene formation, (3), results from ipso substitution of the hydroxyl group by H atom: $H^\bullet + C_6H_5OH \rightarrow C_6H_6 + HO^\bullet$ (22), for which $\log k_{22} = (9.85 \pm 0.15) - (5387 \pm 334 \text{ cal·mol}^{-1})/2.3RT$ was derived based on an equilibrium concentration of $H^\bullet$. Reaction 4 proceeds via phenoxy radicals, formed by $H^\bullet + C_6H_5OH \rightarrow C_6H_5O^\bullet + H_2$ (30), and decomposing via $C_6H_5O^\bullet \rightarrow CO + C_5H_5^\bullet$ (29). No evidence for the previously suggested direct molecular route from phenol to CO and cyclopentadiene (CP) was found; our results show that this route could account for $\leq 7\%$ of CO formation. Based on the reported parameters for (29), a value $\Delta H_f{}^\circ{}_{298}(C_6H_5O^\bullet)_g \approx 9$ kcal·mol^{-1} is derived.

Introduction

We have recently examined the hydrogenolyses of chloroethylene[1] and chlorobenzene.[2] Both substrates were found to be dechlorinated via a mechanism involving hydrogen atoms. In an excess of H_2 at atmospheric pressure, a half-life of 10 s is observed for chlorobenzene at ca. 1030 K, but at ca. 960 K for chloroethylene. Essentially complete levels of dechlorination (99.95%) were obtained in tubular flow reactors in 3-5 s, in the neighborhood of 1200 K. Hydrogenolysis has been shown[3-5] to be a promising method for the treatment of (potentially) toxic industrial waste such as PCB's. Compounds containing functionalities other than chlorine may be present in such waste or be wastes in their own right; their behavior is therefore also of interest.

Phenols are common chemicals and merit special attention as possible precursors for dibenzofurans and dibenzodioxins. As a model for this class, we have chosen to examine the rate and mechanism of phenol thermolysis in H_2 at atmospheric pressure. The high-temperature reactions of phenol are also important in pyrolytic and combustion systems, and this work is additionally of interest from that standpoint.

---

(1) Manion, J. A.; Louw, R. *J. Chem. Soc., Perkin Trans. 2* **1980**, 1047.

(2) Manion, J. A.; Louw, R. *Recl. Trav. Chim. Pays-Bas* **1988**, *107*, 434.

(3) (a) Louw, R.; Dijks, J. H. M.; Mulder, P. *Recl. Trav. Chim. Pays-Bas*, **1984**, *103*, 271. (b) Louw, R.; Dijks, J. H. M.; Mulder, P. *Chem. Ind.* **1983**, 753.

(4) Manion, J. A.; Mulder, P.; Louw, R. *Environ. Sci. Technol.* **1985**, *19*, 280.

(5) US Pat. appl. 770392; Eur. Pat. appl. 85201362.2.

0022-3654/89/2093-3563$01.50/0

There appear to be no previous studies of phenol thermolysis in H_2 or on the reactions of phenol with hydrogen atoms, the chemistry of which is likely to be of importance in this system. There are, however, limited reports on the pyrolysis of phenol. Cypres and Bettens examined phenol[6,7] and cresol[7,8] pyrolyses between 938 and 1138 K. They found carbon monoxide, hydrogen, methane, benzene, cyclopentadiene (CP), naphthalene, and indene as major products. On the basis of deuterium labeling studies, they concluded that CO formation occurred via a molecular elimination reaction after isomerization to a cyclohexadienone intermediate (reactions 1 and 2). Weckman et al.[9] pyrolyzed a phenol/benzene mixture at 1183 K in nitrogen under tank flow conditions, found product distributions similar to those found by Cypres and Bettens, and determined that the pyrolysis was approximately first order in phenol.

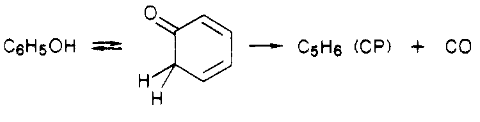

1

(1)

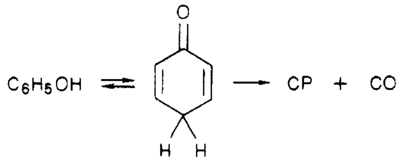

2

(2)

Experimental Section

Apparatus. The apparatus consists of a spiralized quartz tubular flow reactor, 0.4 × 230 cm, effective volume 29.1 mL (a few experiments were conducted in a tank flow reactor, volume 24.5 mL) in an electrically heated oven controlled by a proportional temperature regulator. Temperatures were monitored by several chromel–alumel thermocouples placed over the length of the tubular flow reactor and by two thermocouples at different places within a thermocouple well for the tank flow reactor. A slight systematic temperature variation over the length of the tubular flow reactor was observed (±5 K) and the average temperature was used in this case. Gases were introduced via calibrated flow meters and liquid reagents with an automated syringe.

Chemicals. Phenol (Baker Analysed 99+%) was distilled, liquified with ca. 8 wt % distilled water, degassed, and stored under nitrogen prior to use. C_6D_6 (Aldrich, 99.5 or 99.96+ atom %) was used as such. C_6H_5OD (99.7% D) was purchased (MSD Isotopes, Canada). This material was found to be ca. 6% ortho deuterated (300 MHz NMR) but was used as such. In experiments, the deuteriophenol was handled in a dry glovebox, dissolved in freshly distilled dry benzene, and used immediately. Tank gases (Hoekloos) hydrogen (<5 ppm O_2) and high-purity nitrogen (<3 ppm O_2) were used as such, except in experiments below 975 K, where they were prereacted at ca. 1200 K to remove traces of O_2.

Analytical Procedures. Becker and Hewlett Packard gas chromatographs were used for quantitative analyses. For C_1 and C_2 products, samples of exit gas (0.5 mL) were injected on a Carbosieve B column (Supelco) to which a Chrompack Methanizer was connected (The Methanizer catalytically converts CO and CO_2 to CH_4, allowing FID detection). Conditions: H_2 carrier gas, 30 mL/min; temperature program 120 °C, 12 deg/min, to 220 °C; Methanizer at 380 °C, isothermal. Peak areas were calibrated daily with a 1.00 ± 0.02 vol % standard mixture (Scott Specialty Gases) of CO, CO_2, CH_4, C_2H_2, C_2H_4, and C_2H_6.

At temperatures >1025 K, benzene and other nongaseous products were collected in traps cooled in liquid nitrogen, an internal standard was added, and the benzene was determined by GC/FID analysis (50-m capillary CP-Sil 5 CB WCOT column, 0.32 mm o.d., 0.12 μm film thickness. Conditions: H_2 carrier, 2 mL/min; temperature program 60 °C/6 min, 10 deg/min, to 270 °C, 15 min). Molar responses of compounds were determined from standard mixtures. Small quantities of glass wool were found to improve trapping efficiencies of the volatile benzene and cyclopentadiene products, but small fractions were still found to pass through the trap. These compounds were therefore also analyzed for in the exit gas after coming out of the trap, as above, but by utilizing a 10-m capillary CP-Sil 5 CB WCOT column, 0.53 mm i.d., 0.12 μm film thickness. Conditions: H_2 carrier, temperature program 60 °C/5 min, 10 deg/min, to 150 °C. The following injection procedure was used to remove traces of hydrocarbons from the syringe wall: after injection, with the syringe needle still in the injection port, the plunger was partially withdrawn twice and the gas reinjected. The benzene fraction retained in the cold trap was generally >95% of the total, except at low conversions, where it was as low as 70%. Under these conditions, the above procedure becomes less accurate, due to variations of the trapping efficiency with time. Hence, at temperatures <1025 K, a second method for benzene determination was devised whereby, as an internal standard, ca. 1.5 mol % of C_6D_6 was added to the phenol feed. Assuming equal trapping efficiencies for C_6H_6 and C_6D_6, benzene can be determined by using GC/mass spectrometrical analysis (50-m CP-Sil 5 column, as above, equipped with a HP 5970 MSD) and the relation $C_6H_6/\text{mmol h}^{-1} = (X)(Y)(\text{area M78/area M84})(C_6D_6/\text{mmol h}^{-1})_0$, where $(C_6D_6)_0$ is the feed per hour of the standard and Y is a factor taking into account the relative ionization and fragmentation efficiencies of the respective compounds (determined from standard mixtures, $Y \approx 1.0$). To some extent, C_6D_6 is hydrogenolyzed to give less deuterated benzenes and X accounts for the partial conversion of C_6D_6 (determined in each analysis). As deuterium removal from C_6D_6 was never more than 15% (per site) and turned out to be statistical within experimental error, essentially no C_6H_6 is produced from the standard. This method also allows the accurate determination of the relative rates of desubstitution and dedeuteration of phenol and deuteriobenzene, respectively. We have extended this technique to other substituted benzenes and a complete report will be published elsewhere.[10]

Results

Experiments were carried out at atmospheric pressure between 922 and 1175 K, mostly in the spiralized quartz tubular flow reactor of volume 29.1 mL (230 × 0.4 cm); hydrogen/phenol molar intake ratios were varied between 13 and 200 and residence times were typically 3–4 s. In order to check for surface effects, a limited number of experiments were carried out in a tank flow reactor of 24.5 mL (S/V ratio ca. 1.1 cm^{-1}, or 1/9th of that of the tubular reactor) and, in addition, in the tubular flow reactor, but after treatment with hot 12 N NaOH solution, a procedure which enhances chain termination reactions on the surface.[11]

Preliminary results showed that there were two initial pathways of roughly equal importance in phenol hydrogenolysis, one leading to benzene and water (3), and the other to CO and a C_5 species (model eq 4). The inertness of the water diluent was confirmed

$$H_2 + C_6H_5OH \rightarrow C_6H_6 + H_2O \qquad (3)$$

$$C_6H_5OH \xrightarrow{(H_2)} C_5H_6(CP) + CO \qquad (4)$$

at 1035 and 1096 K by varying the water content between 0 (phenol liquified with a little benzene) and 30 wt %; no changes were observed in the rate constants for either CO or benzene formation.

In addition to benzene and cyclopentadiene (CP), thermolysis of phenol in hydrogen leads to a wide range of organic products. Detailed product distribution data for experiments with a phenol intake concentration of about 6 vol % are presented in Table I

---

(6) Cypres, R.; Bettens, B. *Tetrahedron* **1974**, *30*, 1253.

(7) Cypres, R.; Bettens, B. *Tetrahedron* **1975**, *31*, 359.

(8) Cypres, R.; Bettens, B. *Tetrahedron* **1975**, *31*, 353.

(9) Weckman, E.; Brezinsky, K.; DeMay, J.; Glassman, I. *Chem. Phys. Processes. Combust.* **1983**, Paper No. 35.

(10) Manion, J. A.; Louw, R., to be published.

(11) (a) Kanan, K.; Purnell, H.; Smith, E. *Int. J. Chem. Kinet.* **1983**, *15*, 63. (b) Kanan, K.; Purnell, H.; Smith, E. *Ibid.* **1983**, *15*, 845.

TABLE I: Products in the Thermolysis of ca. 6 vol % C_6H_5OH in Hydrogen[a]

expt no.	1	2	3	4	5	6	7	8	9
temp/K	1017	1028	1038.5	1050.5	1068.5	1083	1109	1130	1147
inflows[b]/(mmol/h)									
H_2	324	292	298	292	298	290	287	287	297
t/s	3.53	3.82	3.72	3.70	3.57	3.62	3.51	3.44	3.21
products[c]/(mmol/h)									
CO	0.84	1.39	1.85	2.62	4.08	6.02	8.37	10.56	12.2
CH_4	0.071	0.12	0.22	0.44	0.90	1.57	3.10	5.02	8.60
C_2H_2	≤0.01	0.011	0.018	0.027	0.061	0.12	0.20	0.29	0.33
C_2H_4	0.068	0.086	0.13	0.24	0.45	0.79	1.46	2.20	4.02
C_2H_6	0.0032	0.0076	0.014	0.034	0.080	0.16	0.40	0.58	1.04
CP	0.48	0.60	0.83	0.89	1.76	1.84	1.21	0.80	0.38
BZ	1.30	1.79	2.32	2.86	4.17	5.34	7.09	7.72	7.36
TOL	0.0022	0.0050	0.010	0.014	0.037	0.069	0.15	0.16	0.13
STYR	0.0021	0.0055	0.0090	0.011	0.021	0.037	0.031	0.028	0.021
C_6H_5OH	17.9	15.8	15.1	13.5	10.7	7.52	3.21	0.60	0.33
IND	0.025	0.056	0.080	0.13	0.26	0.38	0.45	0.42	0.38
NPL	0.045	0.095	0.131	0.20	0.40	0.61	0.84	1.10	1.15
1-Me-NPL	<0.001	0.0013	0.0019	0.0032	0.0062	0.0081	0.011	0.0085	0.0070
2-Me-NPL	<0.001	0.0006	0.0010	0.0016	0.0031	0.0048	0.0075	0.0071	0.0070
BIPH	<0.001	0.0010	0.0015	0.0024	0.0050	0.0080	0.015	0.024	0.034
DBF	0.011	0.012	0.0096	0.0085	0.0076	0.0072	0.0067	0.0061	0.0054
ACE-NPL	<0.001	0.0020	0.0020	0.0032	0.010	0.022	0.053	0.087	0.12
FL	<0.001	0.0021	0.0021	0.0031	0.010	0.017	0.029	0.048	0.061
PHN-AN	<0.001	0.0025	0.0032	0.0044	0.012	0.024	0.037	0.072	0.10
AN	<0.001	0.0018	0.0023	0.0032	0.0091	0.015	0.028	0.056	0.074
%C	102	94.0	97.0	93.9	96.5	92.0	85.1	81.8	87.4
log k(CO)/s^{-1}	−1.889	−1.691	−1.544	−1.370	−1.118	−0.893	−0.578	−0.248	−0.092
log k(BZ)/s^{-1}	−1.699	−1.581	−1.444	−1.331	−1.105	−0.944	−0.650	−0.384	−0.311
log k(22)/M^{-1} s^{-1}	8.692	8.695	8.721	8.712	8.758	8.779	8.832	8.911	8.838

[a] Untreated tubular flow reactor, volume 29.1 mL; atmospheric pressure. [b] Inflows (mmol/h): C_6H_5OH = 19.5, H_2O = 9.1. [c] Based on GC analyses, totals not equal 100%; BZ = benzene; TOL = toluene; STYR = styrene; IND = indene; NPL = naphthalene; 1-Me-NPL = 1-methylnaphthalene; 2-Me-NPL = 2-methylnaphthalene; BIPH = biphenyl; DBF = dibenzofuran; ACE-NPL = acenaphthylene; FL = fluorene; PHN-AN = phenanthrene; AN = anthracene. [d] [H•] assumed to be at equilibrium, calculated from data in ref 16.

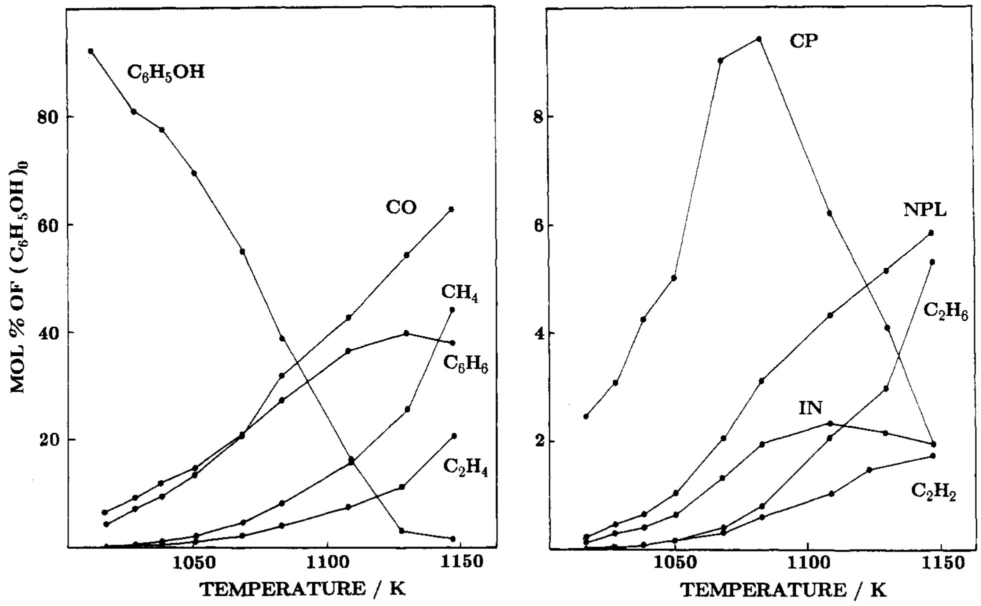

Figure 1. Products in the thermolysis of ca. 6 vol % phenol in H_2. CP = cyclopentadiene, NPL = naphthalene, IN = indene.

and, for major products, in Figure 1. Compound identification was made on the basis of capillary GC retention times compared with authentic samples and confirmed via GC/MSD analysis.

At lower temperatures the dominant products are CO, benzene, CP, and small amounts of indene, naphthalene, and C_1 and C_2 hydrocarbons. Water was also presumed to be a product, but no attempt was made to determine it. Qualitatively, its presence was confirmed by the formation of a bilayer in the product of the phenol/benzene mixture (no water added) at 1096 K. The above compounds remain the primary products throughout the temperature range, except for cyclopentadiene, which passes through a sharp maximum at about 1080 K (Figure 2). At higher temperatures numerous other compounds appear, including C_3–C_5 hydrocarbons, toluene, styrene, fluorene, anthracene, phenanthrene, and trace amounts of other polycyclic aromatic hydrocarbons (PAH's). The only observed organic oxygen-containing compound other than phenol was dibenzofuran (DBF), which was never present in amounts greater than 0.06 mol % of the phenol introduced. Dibenzo-*p*-dioxin, of special interest because of the toxicity of its chlorinated forms, was specifically sought, but not found; on the basis of our detection limits, we estimate that ≤50 ppm could have been formed under our conditions.

In general the mass balance was good, with over 90% of the carbon atoms accounted for (Table I), except at the highest temperatures, where it was typically 85%. We believe the "missing" mass to be present mostly as C_3–C_5 gaseous hydrocarbons, which were noted but not determined, and, at greater conversions, as undetermined PAH's, tar, and small amounts of

TABLE II: Effect of H_2 Concentration on CO and Benzene Formation[a]

expt no.	temp/K	t^b/s	CO/(mmol/h)	C_6H_6/(mmol/h)	log $[H_2]$	log k_{CO}/s^{-1}	log $k_{BZ}{}^c/s^{-1}$
A1[d]	944	4.32	0.0802	e	−1.93	−3.017	e
A2[d]	944	4.28	0.0787	e	−2.18	−3.021	e
A3[d]	944	4.30	0.0793	e	−2.50	−3.020	e
A4[f]	1009	3.97	0.714	1.19	−1.95	−2.013	−1.790
A5[f]	1009	3.96	0.731	0.979	−2.12	−2.002	−1.877
A6[f]	1009	4.07	0.766	0.771	−2.31	−1.998	−1.995
A7[f]	1009	3.92	0.720	0.550	−2.54	−2.011	−2.128
A8[f]	1018	2.93	0.858	1.07	−1.95	−1.801	−1.705
A9[f]	1018	2.93	0.924	0.767	−2.23	−1.772	−1.852
A10[f]	1018	2.97	0.946	0.495	−2.56	−1.770	−2.052
A11[g]	1076	2.86	2.24	1.99	−1.96	−0.978	−1.030
A12[g]	1076	2.80	2.28	1.40	−2.25	−0.981	−1.191
A13[g]	1076	2.87	2.40	1.01	−2.58	−0.977	−1.353
B1[h]	1020	4.06	0.030	e	i	−2.716	e
B2[h]	1021	3.98	0.046	e	−2.22	−2.526	e
B3[h]	1021	3.98	0.016	e	−2.98	−2.970	e

[a] Series A, tubular flow quartz reactor, volume 29.1 mL; series B, same reactor, but treated with hot aqueous NaOH before reaction (see text). [b] Based on measured gas flow out. [c] BZ = benzene. [d] Inflow C_6H_5OH = 19.3 mmol/h. [e] Not determined. [f] Inflow C_6H_5OH = 19.5 mmol/h. [g] Inflow C_6H_5OH = 9.75 mmol/h. [h] Inflow C_6H_5OH = 3.90 mmol/h. [i] N_2 only; H_2 not determined.

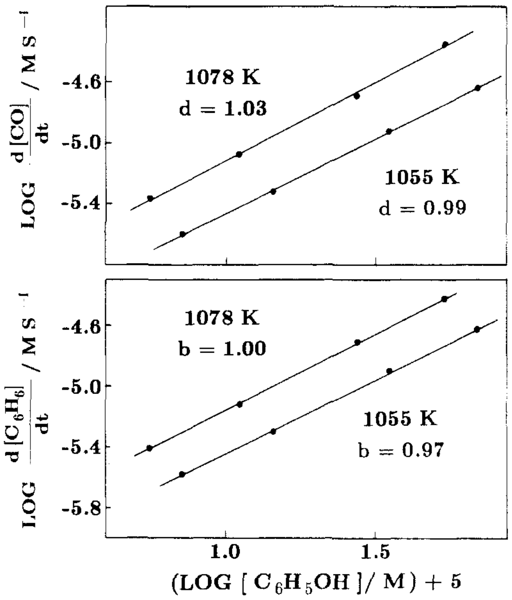

Figure 2. Orders of CO and benzene formation with respect to phenol.

soot. Soot formation, not surprisingly, was heavily dependent on the H_2/phenol intake ratio. At very high ratios, >75, the product appeared to be soot-free even at the highest temperatures; at lower ratios, however, soot particles began to appear in the effluent at temperatures typically above 1100 K.

The stoichiometry of reaction 4 would suggest that CO and CP are being formed at the same rate. The data show, however, that CP/CO < 1, with this ratio decreasing from 0.6 at 1017 K to 0.03 at 1147 K. Apparently CP is undergoing further reaction. We therefore monitored reaction 4 by following the rate of CO formation.

The possibility that CO is itself converted via reactions 5 and 6 must be considered. When mixtures of CO, H_2O, and H_2 were

$$CO + 3H_2 \rightleftarrows CH_4 + H_2O \qquad (5)$$

$$CO + H_2O \rightleftarrows H_2O + CO_2 \qquad (6)$$

reacted under similar conditions, however, CH_4 formation was negligible. CO_2 was determined concomitant with CO and was never >0.4% of the CO value. These traces may, at least in part, be an artifact of the analytical procedure, resulting from contamination of the exit gas sample with air during the injection procedure; whatever the case, CO_2 formation may safely be neglected.

Orders of Reactions and Kinetics. If reactions 3 and 4 are the only important routes to phenol conversion, and if there are no further sources or conversions of CO and benzene, logically, the sum of these three products should equal the phenol introduced. This condition is satisfactorily met at temperatures between 1050 K (with phenol conversion >25%) and 1110 K. At higher temperatures, however, we have reason to believe (vide infra) that some benzene probably results from secondary reactions and that it may therefore no longer be taken as a measure of reaction 1.

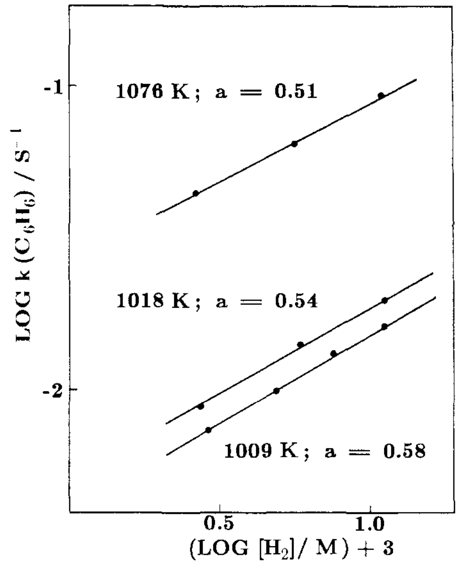

Figure 3. Order of benzene formation with respect to H_2.

The rates of production of benzene and CO may be written as functions of the phenol and hydrogen concentrations:

$$R_{C_6H_6} = k_1[H_2]^a[C_6H_5OH]^b \qquad (7)$$

$$R_{CO} = k_2[H_2]^c[C_6H_5OH]^d \qquad (8)$$

The data presented in Table II and diagrammed in Figure 2 show that the order with respect to phenol is 1 for both products. Assuming (3) and (4) are the only important reactions of phenol, and given that $[H_2]$ is virtually constant under the pseudo-first-order conditions used, the situation reduces to that for two parallel first-order reactions. Under our tubular flow conditions the overall (k_{ov}) and individual rate constants may be defined by

$$k_{ov}/s^{-1} = 1/t \ln (C_6H_5OH)_0/(C_6H_5OH)_t \qquad (9)$$

$$k_{C_6H_6}/s^{-1} = k_{ov}(C_6H_6)_t/(CO + C_6H_6)_t \qquad (10)$$

$$k_{CO}/s^{-1} = k_{ov}(CO)_t/(CO + C_6H_6)_t \qquad (11)$$

In order to determine *a* and *c*, the concentration of H_2 was varied by replacing it with an appropriate amount of nitrogen. Figures 3 and 4 show that benzene formation is about 0.5 order and CO

TABLE III: Rate Data for CO and C_6H_6 Formation in Phenol Thermolysis in H_2[a]

expt no.	temp/K	H_2/(mmol/h)	t^b/s	C_6H_5OH/(mmol/h)	CO/(mmol/h)	C_6H_6/(mmol/h)	log $k_{CO}{}^c$/s^{-1}	log $k_{BZ}{}^c$/s^{-1}	log $k_{22}{}^d$/M^{-1} s^{-1}
A1[e]	1055	310	2.82	14.0	2.46	2.52	−1.287	−1.276	8.715
A2[f]	1055	310	2.94	6.74	1.25	1.33	−1.297	−1.268	8.716
A3[g]	1055	310	3.01	2.66	0.512	0.538	−1.294	−1.272	8.708
A4[h]	1055	310	3.03	1.45	0.266	0.281	−1.277	−1.253	8.726
A5[e]	1078	395	2.77	10.25	4.67	3.99	−0.942	−1.010	8.752
A6[f]	1078	395	2.89	5.33	2.21	2.07	−0.986	−1.014	8.743
A7[g]	1078	395	2.97	2.11	0.886	0.818	−0.997	−1.032	8.722
A8[h]	1078	395	2.97	1.03	0.449	0.417	−0.990	−1.034	8.720
A9[i]	922	272	4.62	*j*	0.0350	0.100[k]	−3.404	−2.948	8.579
A10[l]	934	298	4.38	*j*	0.0250	0.0683[k]	−3.227	−2.790	8.580
A11[l]	952	298	4.35	*j*	0.0543	0.124[k]	−2.885	−2.527	8.616
A12[l]	983	294	4.30	*j*	0.172	0.293[k]	−2.372	−2.142	8.631
A13[l]	995.5	294	4.27	*j*	0.271	0.447[k]	−2.166	−1.949	8.681
A14[l]	1019	287	4.16	*j*	0.544	0.829[k]	−1.841	−1.653	8.719
A15[e]	1034	292	4.04	7.82	0.890	1.14	−1.596	−1.488	8.725
A66[d]	1063	285	3.83	10.89	3.93	3.97	−1.171	−1.167	8.571
A17[e]	1127	291	3.67	0.430	4.80	3.95	−0.359[m]	−0.443	8.879
A18[h]	1136	289	3.98	0.079	1.026	0.804	−0.355[m]	−0.461	8.761
A19[h]	1163	301	3.62	0.0074	1.16	0.911	−0.038[m]	−0.142	8.852
A20[e]	1174.5	382	2.67	0.021	5.70	4.32	0.129[m]	0.0091	8.930
B1[g]	1015	341	3.51	9.42	0.0934	0.118	−2.559	−2.457	7.946
B2[g]	1021	304	4.03	3.95	0.0830	0.0911	−2.267	−2.227	8.103
B3[g]	1021	304	4.03	*j*	0.0271	*j*	−2.763		
C1[f]	1052	302	3.28	6.34	1.31	1.48	−1.317	−1.264	8.744
C2[g]	1072	296	3.34	1.88	0.854	0.869	−1.047	−1.053	8.756

[a] Atmospheric pressure, phenol liquified with ca. 8 wt % water; series A, tubular flow reactor, volume 29.1 mL; series B, series A reactor after treatment with 12 N hot aqueous NaOH; series C, tank flow reactor of effective volume 24.5 mL. [b] Based on measured gas flow out. [c] BZ = benzene; calculated from eq 9–11. [d] Equilibrium H atom concentration assumed; calculated from thermodynamic data in ref 16. [e] C_6H_5OH = 19.5 mmol/h. [f] C_6H_5OH = 9.75 mmol/h. [g] C_6H_5OH = 3.90 mmol/h. [h] C_6H_5OH = 1.95 mmol/h. [i] C_6H_5OH = 19.3 mmol/h; 1.5 mol % C_6D_6 added as internal standard. [j] Not determined. [k] Calculated from eq 5. [l] C_6H_5OH = 9.67 mmol/h; 1.5 mol % C_6D_6 added as an internal standard. [m] Rates calculated directly from experimental phenol outflow.

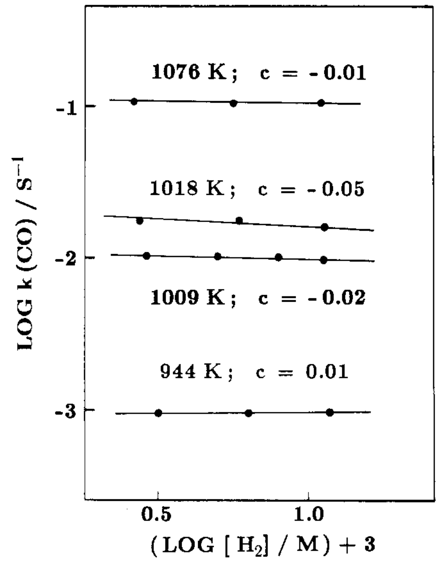

Figure 4. Order of CO formation with respect to H_2.

formation is about zeroth order with respect to H_2. Within experimental error, there was no variance in these orders at phenol conversions as high as 45% and temperatures up to 1076 K, the highest at which they were determined.

For the calculation of rate constants from eq 9, at low to moderate conversions, $(C_6H_5OH)_t \equiv (C_6H_5OH)_0 - (CO)_t - (C_6H_6)_t$. This was done because of severe tailing in the phenol peak in the GC analyses. As a result the standard deviations of the phenol determinations were 2–3 times those for the other compounds. We estimate the GC analytical error in phenol to be ca. 5% compared with ca. 2% for the other compounds. Accordingly, the above method was believed to yield more consistent and accurate results, although in practice the rate constants were not different. At high conversions, when phenol became a relatively small fraction of the sample, tailing was less of a problem; hence, at conversions set somewhat arbitrarily as ≥60%, the phenol value was determined directly from the GC analyses.

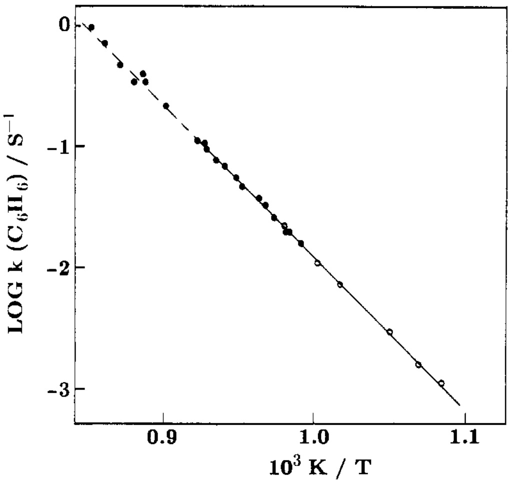

Figure 5. First-order Arrhenius plot for benzene formation in H_2 in untreated reactor between 922 and 1083 K. Data at temperatures above 1083 K are included for comparison but were not used in the analysis because of secondary sources of benzene (see text). Least-squares analysis (errors are 2σ): $k(C_6H_6)/s^{-1} = (10.50 \pm 0.21) - (56758 \pm 840\ \text{cal}\cdot\text{mol}^{-1})/2.3RT$.

Further rate data on benzene and CO are presented in Table III; Arrhenius plots of the data from the untreated reactor are shown in Figures 5 and 6. Between 922 and 1083 K, least-squares analyses yield the following expressions (errors are 2σ):

$$\log k_{C_6H_6}/s^{-1} = (10.50 \pm 0.21) - (56758 \pm 840\ \text{cal}\cdot\text{mol}^{-1})/2.3RT \quad (12)$$

$$\log k_{CO}/s^{-1} = (13.52 \pm 0.22) - (71540 \pm 1044\ \text{cal}\cdot\text{mol}^{-1})/2.3RT \quad (13)$$

Because of secondary sources of benzene, points above 1083 K, while included for comparison, were not used in the determination of the parameters.

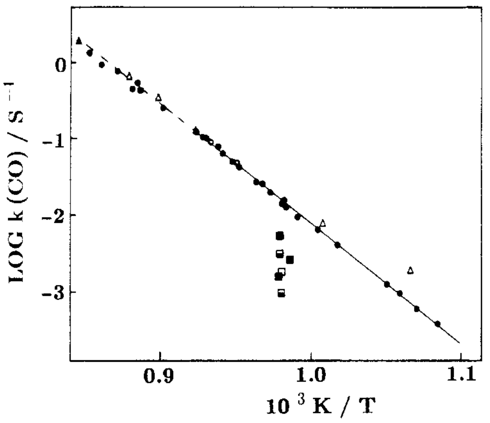

Figure 6. First-order Arrhenius plot for CO formation from phenol. Results under pyrolytic conditions from ref 6 and 9 are also included. (●) Untreated tubular flow reactor, H_2 only; (○) untreated tank flow reactor, H_2 only. Tubular flow reactor after treatment with 12 N aqueous NaOH: (■) H_2 only; (◧) H_2/N_2; (□) N_2 only; (▲) pyrolysis, ref 9; (△) pyrolysis, calculated from ref 6, assuming tank flow conditions. Least-squares analysis of data in untreated tubular flow reactor (errors are 2σ): $\log k_{CO}/s^{-1} = (13.52 \pm 0.22) - (71540 \pm 1044\ \text{cal·mol}^{-1})/2.3RT$.

TABLE IV: Deuterium Content (%) of Hydrogenolysis Products of C_6H_5OH/C_6D_6 Mixture[a]

no. of deuteriums	products[b]					
	C_6H_5OH[c]	CP	TOL	STYR	IND	NPL
1	0.4	0.4	0.3	<0.3	<0.3	<0.3
>1	<0.3	<0.3	<0.3	<0.3	<0.3	<0.3

[a] Untreated tubular flow reactor; 1019 K, inflows/(mmol/h): H_2O = 292, C_6H_5OH = 17.1, C_6D_6 = 4.0; t = 4.0 s. [b] CP = cyclopentadiene; TOL = toluene; STYR = styrene; IND = indene; NPL = naphthalene. [c] Refers to ring hydrogens only due to exchange of hydroxyl hydrogen.

Experiments with Deuterated Compounds. In order to facilitate mechanistic interpretation of the data, two sets of experiments were performed with deuterated compounds.

In the first, a mixture of phenol and C_6D_6 was reacted at 1008 K and the products checked for deuterium content via GC/MSD analysis (Table IV). As dedeuteration of C_6D_6 is relatively minor under these conditions (<15%, per site),[10] compounds stemming from benzene should show a heavily deuterated fraction. No deuterium was found in the styrene, indene, or naphthalene, while monodeuterated phenol, CP, and toluene were found near the limit of detection (ca. 0.3%). Other than deuteriobenzenes, no compounds containing more than one D atom were found.

For the second experiment, C_6H_5OD in dry benzene was reacted at 529, 910, and 1004 K and the recovered phenol checked for deuterium incorporated into the phenyl ring. This would be expected if reversible formation of the cyclohexadienone isomers of phenol were occurring (reactions 1 and 2). At the two highest temperatures, product analysis by GC/MSD and 300-MHz NMR show that small amounts of the hydroxyl deuterium have been incorporated into the phenyl ring, although interestingly only in the ortho position. The deuterium content of CP was also examined; only a small portion (13–15%) was found to be deuterated.

Influence of Reactor Surface and S/V Ratio. The possible influence of the reactor surface on the reaction is of interest. Despite a nearly 10-fold difference in the S/V ratio, rate constants obtained in a tank flow reactor were, within experimental error, the same as those found under tubular flow conditions (Table III, experiments C1–C2). The surfaces in both reactors were clean quartz. Because of the generally high H_2/phenol ratio, buildup of a carbon layer was avoided.

In contrast, when the tubular flow reactor was treated with concentrated aqueous sodium hydroxide as described by Kanan et al.,[11] formation rates of both CO and benzene were reduced 2–15-fold, although the ratio of these rates was hardly changed (Table II, experiments B1–B3; Table III, experiments B1–B3). This system was also found to exhibit variable behavior, including irreproducible results, an induction period, and memory effects. As will be later discussed, we believe these effects arise from rapid chain termination steps occurring on the surface; in any case, the inconsistent behavior makes this system ill-suited for a detailed study.

Discussion

Major Pathways and Secondary Reactions. The product distribution curves show that reactions 3 and 4, resulting in CO and CP, and benzene and water, are by far the most important pathways in the thermolysis of phenol in H_2. The fact that the CP curve (Figure 2) goes through a sharp maximum indicates that it reacts further and is likely to be responsible for many of the other products. Benzene might also be involved in the formation of indene, naphthalene, etc., but the results of the phenol/C_6D_6 experiments (Table V) do not support this. Because dedeuteration of C_6D_6 is minor under these conditions,[10] all products stemming from it should be heavily deuterated. At 1008 K, this is cnearly not the case for the examined products: indene, naphthalene, styrene, and toluene. Unfortunately, due to increasing dedeuteration of C_6D_6, this technique could not be extended to higher temperatures. The traces of monodeuterated phenol, CP, and toluene are probably accounted for by D atoms, produced in the dedeuteration of C_6D_6, which can deuterate unsaturated centers via a hydrogen displacement mechanism.

Naphthalene and indene are likely to arise from the overall reactions of two CP molecules, probably involving the reaction between two CP-derived radicals or of a CP-derived radical with CP. These processes are shown as the formal stoichiometries (14) and (15). Mechanistic pathways are detailed elsewhere.[12] At 1017 K, based on CO formation, some 10% of the CP formed ultimately ends up as naphthalene, while by 1147 K this has risen to 20% (Table I, experiments 1 and 9). The indene/naphthalene ratio is initially almost constant, rising from 0.56 at 1017 K to 0.65 at 1068 K; thereafter this ratio drops until it is 0.3 at 1147 K (Table I, experiments 1, 5, and 9). This suggests that indene is less thermally stable than naphthalene and is being further converted; one reasonable pathway is put forth in reactions 16–18.

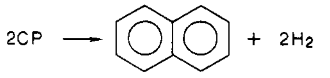

(14)

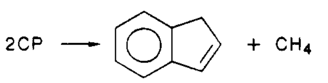

(15)

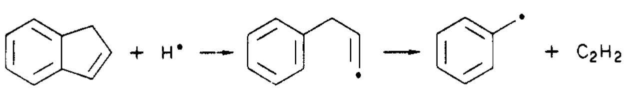

(16)

$$C_6H_5CH_2^{\bullet} + XH \rightarrow C_6H_5CH_3 + X^{\bullet} \quad (17)$$

$$C_6H_5CH_3 + H^{\bullet} \rightarrow C_6H_6 + CH_3^{\bullet} \quad (18)$$

The result of these reactions is to convert indene into toluene and, ultimately, benzene.

The above is one possible route to benzene and there may well be others. In any case, in the hydrogenolysis of CP (CP:H_2 = 1:9 M, $t \approx 7$ s, under tank flow conditions) we have observed[12] ca. 85% conversion of CP at ca. 1050 K, with a selectivity to benzene and toluene of 9 and 2.5%, respectively. The selectivity will very likely decrease with the CP/H_2 ratio, and these reactions will therefore be less important under our conditions (CP/H_2 typically $\leq 10^{-2}$), but, regardless, it is clear that reactions other than (3) may contribute to benzene formation. While these still amount to a relatively minor fraction of the total benzene, they could affect rate parameters at higher conversions, where their influence is greater.

---

(12) Klinkenberg, W.; Louw, R. *C.C.E. Special Report Series*. Leiden University: Leiden, 1987; No. 87-01.

TABLE V: Deuterium Position after Hydrogenolysis of C_6H_5OD[a]

sample	temp/K	t/s	% C_6H_5OD	% ring D[b]	ortho[c]	meta[c]	para[c]	% C_5H_5D[d]
starting mixture	293		≥62[e]	6.0 (8.7)	8.5	0	0.2	*f*
1	529	5.24	*g*	6.6 (*g*)	*h*	*h*	*h*	*f*
2	910	4.43	*g*	23 (21)	21	0	~0	15
3	1004	4.08	*g*	17 (15)	15	0	~0	13

[a] Untreated tubular flow reactor, ca. 50/50 mixture C_6H_5OD/C_6H_6, ca. 1 vol % C_6H_5OD in H_2. [b] Determined from GC/MSD analysis and 300-MHz NMR (parentheses). [c] From relative integrals of 300-MHz ^1H NMR; meta position assumed undeuterated. [d] From GC/MSD. [e] From NMR in $CDCl_3$ (total OH integral). [f] Not present. [g] Not determined due to rapid exchange of hydroxyl hydrogen. [h] Not determined.

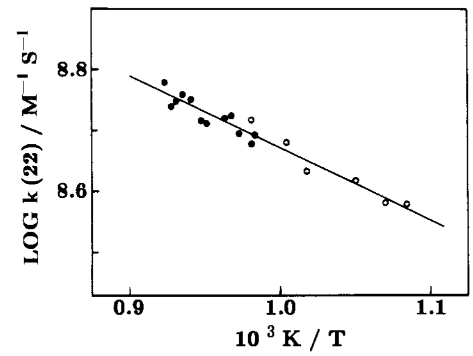

Figure 7. Arrhenius plot for $H^\bullet + C_6H_5OH \rightarrow C_6H_6 + {}^\bullet OH$, assuming equilibrium concentration of $H^\bullet$: (●) benzene determined from GC/FID analysis; (○) benzene determined from GC/MS analysis with C_6D_6 as internal standard (see text). Least-squares analysis (errors are 2σ): $\log k_{22}/M^{-1}\ s^{-1} = (9.85 \pm 0.15) - (5387 \pm 334)\ \text{cal}\cdot\text{mol}^{-1}/2.3RT$.

Formation of Benzene from Reaction 3. Hydrogen atoms may arise and disappear via numerous radical/molecule reactions. In the hydrogenolyses of toluene and propene, Benson[13] has suggested that this will lead to an equilibrium H atom concentration, an assertion supported by recent studies by Robaugh and Tsang[14] on reaction 18. Cao and Back[15] have suggested that wall reactions may also play a role in the equilibration process. The net result may be summarized by model eq 19. The bulk of our results

$$H_2 \underset{}{\overset{[M]}{\rightleftharpoons}} 2H^\bullet \qquad (19)$$

support this proposition; in the following discussion, we will accept this as true and thereafter examine the present evidence with regard to this question.

Hydrogen atom attack on phenol can lead to benzene via two mechanistic pathways, the first involving direct abstraction of the hydroxyl group, followed by reaction of the resulting phenyl radical (reactions 20 and 21), and the second via an addition/elimination sequence, (22) and (23). Cypress and Bettens[7] have proposed

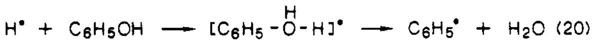

$$H^\bullet + C_6H_5OH \longrightarrow [C_6H_5\text{-}\overset{H}{O}\text{-}H]^\bullet \longrightarrow C_6H_5^\bullet + H_2O \qquad (20)$$

$$C_6H_5^\bullet + H_2 \longrightarrow C_6H_6 + H^\bullet \qquad (21)$$

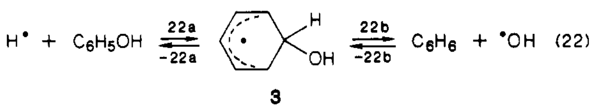

$H^\bullet + C_6H_5OH \underset{-22a}{\overset{22a}{\rightleftharpoons}}$ **3** $\underset{-22b}{\overset{22b}{\rightleftharpoons}} C_6H_6 + {}^\bullet OH$ (22)

3

$$^\bullet OH + H_2 \longrightarrow H_2O + H^\bullet \qquad (23)$$

the former pathway. Both schemes yield a rate expression $R(C_6H_6) = k[H^\bullet][C_6H_5OH]$. If (19) is at equilibrium, $[H^\bullet] = K_{19}^{1/2}[H_2]^{1/2}$, and $R(C_6H_6) = kK_{19}^{1/2}[H_2]^{1/2}[C_6H_5OH]$. Benzene formation was observed to be ca. 0.5 order in H_2 (Figure 3), which is consistent with the equilibrium assumption. Further, a 10-fold change in the phenol concentration had no effect on the rate constant for benzene formation, indicating no concomitant shift in $[H^\bullet]$; this is likely to be true only if $[H^\bullet]$ is virtually at equilibrium.

In Figure 7, the equilibrium H atom concentrations, calculated from the thermodynamic data,[16] have been divided out of the overall rate constants, resulting in an Arrhenius plot for conversion of phenol to benzene by H atom. Although there is still no a priori reason to choose one mechanism over the other, the low 5.4 kcal·mol^{-1} activation energy would seem to disfavor direct abstraction of the hydroxyl group (20), involving, as it does, a presumably high-energy transition state in which the oxygen atom has expanded its octet. Direct abstraction of hydroxyl functions has been proposed in hydroperoxy systems,[17] but there is controversy over this[18] and these involve quite different and much weaker bonds. In the much more closely related case of methanol, Hoyermann et al.[19] have shown that, although H atoms react with CH_3OH with a rate similar to that reported here for phenol, hydroxyl abstraction is negligible up to 680 K, the highest temperature studied. In fact, we would expect OH abstraction from phenol to be even less favored, as its C–OH bond is ca. 20 kcal·mol^{-1} stronger than that of CH_3OH. Hence, the displacement mechanism, (22) and (23), is to be preferred and therefore (errors are 2σ and are a measure of precision only):

$$\log k_{22}/M^{-1}\ s^{-1} = (9.85 \pm 0.15) - (5387 \pm 334\ \text{cal}\cdot\text{mol}^{-1})/2.3RT$$

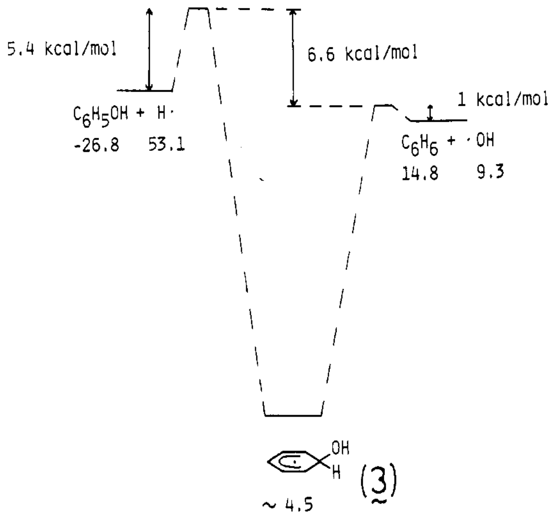

Figure 8. Energy diagram for $H^\bullet + C_6H_5OH \rightarrow C_6H_6 + {}^\bullet OH$ at 1000 K. Heats of formation from ref 15 and 25. $\Delta H_f°(3)$ is calculated from $\Delta H_f°(C_6H_7^\bullet)$,[21] with group additivity contribution derived from comparison of cyclohexane and cyclohexanol; $\log k_{-22b} = (9.66 \pm 0.30) - (1050 \pm 400\ \text{cal}\cdot\text{mol}^{-1})/2.3RT$ (ref 22).

This result, though based on the equilibrium assumption for reaction 19, seems quite reasonable. It is, for example, very similar to that reported for toluene,[14] $\log k_{18} = 10.08 - 5.12$ kcal·mol^{-1}/2.3RT and is also perfectly compatible with the parameters for H atom addition to benzene, $\log k(\text{per site})/M^{-1}\ s^{-1} = 9.87 - 4.3$ kcal·mol^{-1}/2.3RT.[20] Further, from the limited number of

---

(13) Benson, S. W.; Shaw, R. *J. Chem. Phys.* **1967**, *47*, 4052.

(14) Robaugh, D.; Tsang, W. *J. Phys. Chem.* **1986**, *90*, 4159.

(15) (a) Cao, J.-R.; Back, M. H. *Can. J. Chem.* **1982**, *60*, 3039. (b) Cao, J.-R.; Back, M. H. *Ibid.* **1984**, *62*, 86.

(16) *JANAF Thermochemical Tables*, 2nd ed.; Stull, D. R.; Prophet, H., Project Directors; NSRDS-NBS-37, National Bureau of Standards: Washington, DC, 1971.

(17) (a) Klemm, R. B.; Payne, W. A.; Stief, L. J. *Int. J. Chem. Kinet.* **1975**, *S1*, 61. (b) Slemr, F.; Warneck, P. *Int. J. Chem. Kinet.* **1977**, *9*, 267.

(18) Albers, E. A.; Hoyermann, K.; Wagner, H. Gg.; Wolfrum, J. *Symp. (Int.) Combust.* **1971**, *13*, 81–88.

(19) Hoyermann, K.; Sievert, R.; Wagner, H. Gg. *Ber. Bunsen-Ges. Phys. Chem.* **1981**, *85*, 149.

SCHEME I

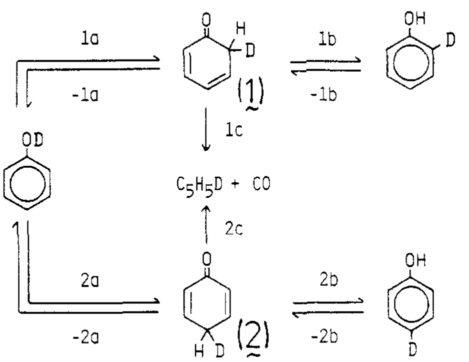

experiments with C_6D_6, we were able to obtain an activation energy of ca. 4.0 kcal·mol^{-1} for the process $H^• + C_6D_6 \rightarrow C_6D_5H + D^•$, again in excellent agreement with the addition parameters. This will be dealt with more completely in a forthcoming article on relative rates of H atom attack on substituted benzenes.[10]

Note that $k_{22} = k_{22a}k_{22b}/(k_{22b} + k_{-22a})$ and refers to the overall rate. If the hydroxycyclohexadienyl intermediate, **3**, were to decompose quasi-exclusively to benzene and $^•OH$, we could identify this directly with the rate of H atom addition (22a). Assuming, for the moment, that $E_{22} \approx E_{22a}$, the energy diagram for (22) at 1000 K is as shown in Figure 8. Thus, $E_{-22a} - E_{22b} \approx 6500$ cal·mol^{-1}. From transition-state theory, $\log (A_{22a}A_{22b}/A_{-22a}A_{-22b}) = \Delta S_{22}/2.3R$. Taking $\log A_{22a}/\mathrm{M}^{-1}\ \mathrm{s}^{-1} = 9.85$, $\log A_{22b}/\mathrm{M}^{-1}\ \mathrm{s}^{-1} = 9.66$,[23] and the entropies from ref 16 and 24, we find $\log (A_{-22a}/A_{22b}) = 9.85 - 9.66 - 1.17/2.3R = -0.07$. Therefore, at 1000 K, $\log (k_{-22a}/k_{22b}) = -0.07 - 6700\ \mathrm{cal{\cdot}mol^{-1}}/2.3RT$. At the mean temperature of our experiments, 1017 K, we calculate that only about 3% of **3** should return to $H^•$ and phenol. Using this result, we may make an improved estimate of A_{22a} and E_{22a} and repeat the calculation; the results converge, yielding

$$\log k_{22a}/\mathrm{M}^{-1}\ \mathrm{s}^{-1} = 9.90 - 5540\ \mathrm{cal{\cdot}mol^{-1}}/2.3RT$$

Some care must be taken with this result as it relies on the extrapolated parameters for k_{-22b} and, although this reaction has been studied often,[23] they could still be subject to some error.

From microscopic reversibility, we may also calculate the overall rate of hydroxyl radical displacement of a benzene hydrogen to give phenol, a process which has been suggested to be of importance in the high-temperature chemistry of benzene:[24]

$$\log k_{-22}/\mathrm{M}^{-1}\ \mathrm{s}^{-1} = 9.58 - 7637\ \mathrm{cal{\cdot}mol^{-1}}/2.3RT$$

As the thermochemistry of all species involved in this calculation is reasonably well-known,[16,25] this result should have an accuracy close to that for the rate constant in the forward direction.

Mechanism of CO Formation. Cypres and Bettens[6] have proposed that molecular reactions 1 and 2 are responsible for CO formation when phenol is pyrolyzed. Logically, these processes, if correct, must also occur in H_2 and we note (Figure 6) that rate constants for CO formation derived from their data are very similar to ours in the untreated reactor.

Scheme I shows that, after reaction of C_6H_5OD, the recovered phenol will be partially ring deuterated if reversible formation of cyclohexadienones is occurring. Deuterium is indeed found in the ortho ring position (Table V), indicating that intermediate **1** is being formed. This is not unreasonable, as $\Delta H_f{}^\circ{}_{298}(\mathbf{1})_g = -17$ kcal·mol^{-1},[26] only 6 kcal·mol^{-1} less stable than phenol itself. The absence of para deuterium implies that hydrogen transfer to this site via (2) is a much slower process, even though **2** is also quite stable, with $\Delta H_f{}^\circ{}_{298}(\mathbf{2})_g = -13$ kcal·mol^{-1}.[26] Apparently the rigidity of the phenyl ring inhibits the shift in this case. It also suggests that direct interconversion of **1** and **2** does not readily occur. [Strictly speaking, the NMR results (Table V) show only that the meta/para positions have equal deuterium contents, while that of ortho is higher. In conjunction with the MS analyses, however, which show that the total D content can be accounted for by the ortho position, we conclude that meta and para positions are *both* undeuterated. The above statement follows from this result.]

As the phenol in the C_6H_5OD experiments was at least 62% hydroxyl deuterated (Table V), the recovered phenol should be ≥41% ring deuterated at equilibrium, if one assumes a statistical distribution between the hydroxyl group and the two ortho positions. The experimental value is only about 0.5 of this at 910 K and even less at 1004 K. It seems that equilibrium is not fully established, and/or that other reactions are removing D from phenol. The somewhat lower D content at 1004 K supports the latter speculation, as the equilibration rate is obviously higher at the higher temperature. Addition and abstraction reactions involving $H^•$ may be partly responsible for this. Regardless, formation of **1** is demonstrably occurring.

Scheme I also shows that all CP derived molecularly from C_6H_5OD will initially be deuterated, yet the D content of CP is only 13–15%. Even allowing for possible removal of D from phenol molecules, the D content of CP should be a minimum of 1.5 times that found in the phenyl ring of the remaining phenol. [The factor 1.5 results from the fact that, due to rapid exchange of the hydroxyl proton prior to analysis, the measured D content in the unconverted phenol refers to ring deuterium only. We have assumed that this represents only 2/3 of the original D content, all of which should be observed in the CP product.] In fact, it is not even equal. Various processes, such as those shown in reactions 24–27, may lower the D content of CP after reaction.

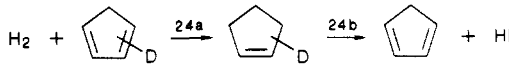

(24)

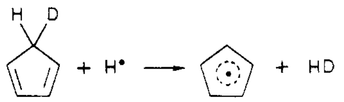

(25)

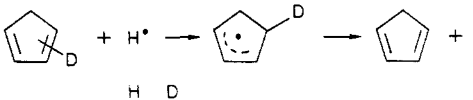

(26)

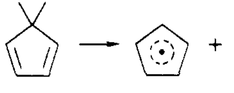

(27)

However, all of these should be retarded by rapid scrambling of D throughout the ring by 1,5-sigmatropic shifts.[27] The rate of (24) can be calculated from the reported rate of (24b),[28] and the rates of (25–27) can be reasonably well estimated. These estimations show that, combined, ≤1% of the CP D should be exchanged at 910 K. Hence, the lack of deuterated CP indicates that CP is not formed by reactions 1c and 2c.

In sum, although gas-phase formation of **1** is apparently occurring, we find no evidence that this intermediate is responsible for CO production.

This conclusion may be confirmed and reached in a simpler manner from the experiments with the NaOH treated reactor. In this reactor, CO formation was up to a factor of 15 slower than in the untreated reactor (Table II, experiment B3). Clearly, a direct gas-phase molecular process would be unaffected by a

---

(20) Nicovich, J. M.; Ravishankara, A. R. *J. Phys. Chem.* **1984**, *88*, 2534.

(21) Tsang, W. *J. Phys. Chem.* **1986**, *90*, 1152.

(22) Tully, F. P.; Ravishankara, A. R.; Thompson, R. L.; Nicovich, J. M.; Shah, R. C.; Kreutter, N. M.; Wine, P. H. *J. Phys. Chem.* **1981**, *85*, 2262.

(23) Atkinson, R. *Chem. Rev.* **1985**, *85*, 69 and references cited therein.

(24) Hsu, D. S. Y.; Lin, C.-Y.; Lin, M. C. *Symp. (Int.) Combust.*, [*Proc.*], *20th* **1985**, *20*, 623.

(25) Stull, D. R.; Westrum, Jr., E. F.; Sinke, G. C. *The Chemical Thermodynamics of Organic Compounds*; Wiley: New York, 1969.

(26) Shiner, C. S.; Vornham, P. E.; Kass, S. R. *J. Am. Chem. Soc.* **1986**, *108*, 5699.

(27) (a) Roth, W. *Chimia* **1966**, *20*, 229. (b) Roth, W. *Tetrahedron Lett.* **1964**, *17*, 1009.

(28) Benson, S. W.; O'Neil, H. E. *Kinetic Data on Gas Phase Unimolecular Reactions*; NSRDS-NBS-21, National Bureau of Standards: Washington, DC, 1970.

change in the surface. This places a maximum of 7% on the quantity of CO that could be formed molecularly from phenol. From the facts that the CO/C_6H_6 ratio was nearly the same in both systems, and that benzene is formed by radical processes, we conclude that CO formation via (1c) and (2c) is insignificant under our conditions. As rate constants for CO formation in N_2 are similar to ours, this conclusion must also apply to phenol pyrolysis at temperatures in the neighborhood of 900–1100 K.

A radical mechanism is the most reasonable alternative and will quite easily explain the surface effect of the treated reactor; it must, however, account for the apparent zero order of the reaction with respect to hydrogen. Phenoxy radical is known to undergo decomposition to CO and cyclopentadienyl radical at elevated temperatures[29,30] and reactions 28 and 29 must therefore be considered. The rate of (28) is unknown, but a reasonable

$$C_6H_5OH \rightarrow C_6H_5O^\bullet + H^\bullet \qquad (28)$$

$$C_6H_5O^\bullet \rightarrow C_5H_5^\bullet + CO \qquad (29)$$

estimate can be made. Values of 9–12.8 kcal·mol^{-1} have been reported for $\Delta H_f{}^\circ{}_{298}(C_6H_5O^\bullet)_g$.[29,30] We favor a value of about 9.2 kcal·mol^{-1} (Appendix), which, using the $C_p{}^\circ$ data of ref 29, leads to $\Delta H(28)$ = 85.8 kcal·mol^{-1} at 1000 K. If we assume $k_{-28}/M^{-1}\,s^{-1} \approx 10^{11}$, similar to that for $CH_3^\bullet + H^\bullet$,[32] and close to the maximum predicted by collision theory, we find $A_{28}/s^{-1} = 10^{14.8}$. Alternatively, we may estimate the A factor by analogy with $C_6H_5CH_3 \rightarrow C_6H_5CH_2^\bullet + H^\bullet$, which (after a symmetry correction) has a ΔS term similar to ΔS_{28}, and has an A factor (per H) of 15.0.[28] Taking the average of these two results, we estimate $\log k_{28}/s^{-1} \approx 14.9 - 83.8\ \text{kcal·mol}^{-1}/2.3RT$. Assuming all $C_6H_5O^\bullet$ species decompose exclusively via (29), we calculate, at 1000 K, a maximum rate constant for CO formation of $10^{-3.5}$ s^{-1}, almost a factor of 30 lower than that observed.

We are not faced with a paradox: CO formation is apparently zero order in H_2, yet (1) it is demonstrably not a molecular reaction; (2) the S/V ratio does not affect the rate, so it does not seem to be a heterogeneous reaction; and (3) the only reasonable unimolecular radical mechanism is far too slow to account for the observed rate of CO formation.

Phenoxy radical still seems to be the most logical CO precursor, but it must arise in another manner, most likely via (30). Making

$$H^\bullet + C_6H_5OH \rightarrow C_6H_5O^\bullet + H_2 \qquad (30)$$

the steady-state assumption for phenoxy radical, and using the equilibrium expression $[H^\bullet]/M^{-1} = K_{19}{}^{1/2}[H_2]^{1/2}$, the following rate law must hold:

$$R_{CO} = k_{29}k_{30}/(k_{-30}[H_2] + k_{29})K_{19}{}^{1/2}[H_2]^{1/2}[C_6H_5OH] \qquad (31)$$

Two limiting cases are then apparent: case 1, $k_{29} \gg k_{-30}[H_2]$, which leads to $R_{CO} = k_{30}K_{19}{}^{1/2}[H_2]^{1/2}[C_6H_5OH]$, and case 2, $k_{29} \ll k_{-30}[H_2]$, for which $R_{CO} = k_{29}K_{30}K_{19}{}^{1/2}[H_2]^{-1/2}[C_6H_5OH]$. These two cases represent extremes of "expected" rates of CO formation via a hydrogen-abstraction mechanism. The first requires knowledge of k_{30}, which is unknown, and the second requires knowledge of k_{29}, which has been reported by Lin and Lin[30] as $\log k_{29}/s^{-1} = 11.4 - 43.9\ \text{kcal·mol}^{-1}/2.3RT$, and of the thermodynamic properties of phenoxy radical, which have been reported, but are still somewhat uncertain. Both situations lead to a rate dependence on the H_2 concentration, 0.5 order for case 1, and −0.5 order for case 2. If, however, the situation were to lie between these two extremes, intermediate behavior would be expected and an order of near zero could be obtained. In the following analysis we will argue that this is in fact the case; further, using this model, we will show that near-quantitative agreement with experiment can be obtained.

TABLE VI: Reactions Used in the Modeling of CO Formation[a]

reaction no.	reaction	log A^b	E^b
22	$C_6H_5OH + H^\bullet \rightarrow C_6H_6 + {}^\bullet OH$	9.85	5.39
28	$C_6H_5OH \rightarrow C_6H_5O^\bullet + H^\bullet$	14.9	83.8
29	$C_6H_5O^\bullet \rightarrow C_5H_5^\bullet + CO$	11.4	43.9
30[c]	$C_6H_5OH + H^\bullet \rightarrow C_6H_5O^\bullet + H_2$	10.2	6.1
−30[c]	$C_6H_5O^\bullet + H_2 \rightarrow C_6H_5OH + H^\bullet$	9.96	26.6

[a] Tubular flow reactor; C_6H_5OH = 2 vol % in H_2, t = 3 s; $[H^\bullet]$ assumed to be at equilibrium, calculated from data in ref 16. [b] Units: s, mol, kcal, L, K. [c] Data correspond to $\Delta H_f{}^\circ{}_{298}(C_6H_5O^\bullet)_g$ = 9.2 kcal/mol.

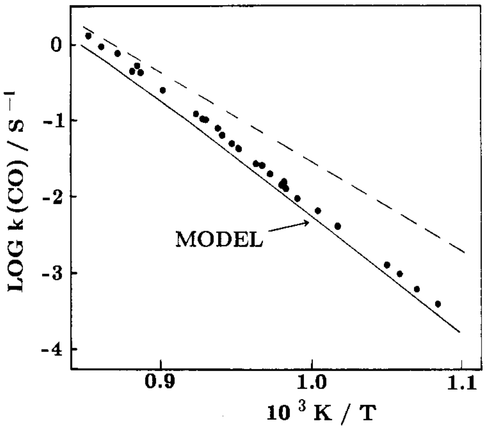

Figure 9. Experimental rate constants for CO formation compared with those modeled using a hydrogen abstraction mechanism. Dashed line is maximum rate constant based on estimated k_{30} and assumption that all $C_6H_5O^\bullet$ species decompose via (29). Solid line is that modeled from reactions and parameters in Table VI.

We begin by estimating k_{30}, which will determine the maximum possible rate of CO formation due to H abstraction. Noting first that H abstractions are in general favored by polar transition states, we propose that k_{30} should fall between that for H abstraction by $H^\bullet$ from HCl,[33] for which $\log k/M^{-1}\,s^{-1} = 10.0 - 3.5\ \text{kcal·mol}^{-1}/2.3RT$, and that for C_2H_6,[34] for which $\log k(\text{per H}) = 10.4 - 9.6\ \text{kcal·mol}^{-1}/2.3RT$. [There is good experimental evidence that oxygen-centered radicals stabilize H-transfer transition states relative to carbon-centered radicals; note, for instance, that $MeO^\bullet + RH \rightarrow R^\bullet + MeOH$ reactions have activation energies typically about 60% of those for the analogous $Me^\bullet + RH$ reaction.[35] The same source shows that the effect is smaller than for transition-states involving chlorine.] We therefore estimate $\log k_{30}/M^{-1}\,s^{-1} \approx 10.2 - 6.0\ \text{kcal·mol}^{-1}/2.3RT$. [BSBL calculations, which provide fairly accurate estimates for a wide variety of H-transfer reactions,[36] suggest the not too different parameters, $\log k/M^{-1}\,s^{-1} = 10.7 - 8\ \text{kcal·mol}^{-1}/2.3RT$ for the reaction $H^\bullet + MeOH \rightarrow MeO^\bullet + H_2$. The phenolic O–H bond is about 20 kcal·mol^{-1} weaker than in MeOH, however, and we prefer our semiempirical approach.] From the thermodynamic data,[16] $\log [H^\bullet]_{eq}/M^{-1} = 0.62 - 51.14\ \text{kcal·mol}^{-1}/2.3RT$ for H_2 = 1 atm, which entails $\log k_{CO}(\text{max}) = 10.8 - 57\ \text{kcal·mol}^{-1}/2.3RT$. Figure 10 shows a comparison of this expression with the experimental points; the above parameters lead to rate constants higher than the measured values, but if some phenoxy radicals return to phenol via (−30), the observed rate will be lower than that for H abstraction.

Using our earlier value for $\Delta H_f{}^\circ{}_{298}(C_6H_5O^\bullet)_g$, and taking the other thermodynamic parameters from Colussi et al.,[29] we calculate $K_{28}(1000\ \text{K}) = 0.24 + 20.5\ \text{kcal·mol}^{-1}/2.3RT$. Using this ex-

---

(29) Colussi, A. J.; Zabel, F.; Benson, S. W. *Int. J. Chem. Kinet.* **1977**, *9*, 161.

(30) Lin, C.-Y.; Lin, M. C. *J. Phys. Chem.* **1986**, *90*, 425.

(31) DeFrees, D. J.; McIver, Jr., R. T.; Hehre, W. J. *J. Am. Chem. Soc.* **1980**, *102*, 3335 and references cited therein.

(32) (a) Patrick, R.; Pilling, M. J.; Rogers, G. J. *Chem. Phys.* **1980**, *53*, 279. (b) LeBlanc, J. F.; Pacey, P. D. *J. Chem. Phys.* **1985**, *83*, 4511 and references cited therein.

(33) Miller, J. C.; Gordon, R. J. *J. Chem. Phys.* **1981**, *75*, 5305.

(34) Cao, J.-R.; Back, M. H. *Int. J. Chem. Kinet.* **1984**, *16*, 961.

(35) Kerr, J. A., Moss, S. J., Eds. *CRC Handbook of Bimolecular and Termolecular Gas Reactions*; CRC Press: Boca Raton, FL, 1981; Vol. 1.

(36) Bērces, T.; Dombi, J. *Int. J. Chem. Kinet.* **1980**, *12*, 183.

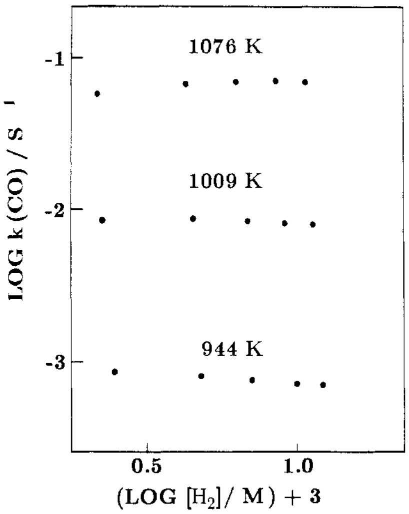

Figure 10. Modeled orders of CO formation with respect to H_2. Based on reactions and parameters in Table VI.

pression and our previous estimation of k_{30}, we find log k_{-30}/M^{-1} s^{-1} = 9.96 − 26.5 kcal·mol^{-1}/2.3RT. This leads, at 1000 K, to $k_{29}/k_{-30}[H_2] = 0.4$, which is exactly what is necessary to obtain intermediate behavior.

A computer model, using the expressions given in Table VI, results in the model rate constant line for CO formation shown in Figure 9. The model line is about 0.15 log units lower than the experimental points but leads to an apparent activation energy of 70.5 kcal·mol^{-1}, in very good agreement with that observed, 71.5 kcal·mol^{-1}.

There are several possible explanations for the slight discrepancy between experiment and model: (1) the thermodynamic properties (ΔH_f°, S°, C_p°) of phenoxy are incorrect, (2) k_{29} is larger (about 0.2 log units) than that inferred from the parameters used, (3) there is a systematic error in temperature (about 10 K), or (4) the steady-state concentration of $H^\bullet$ is above that for equilibrium (about 0.15 log units). Unfortunately, it is not possible to choose which, or which group of these, is most likely responsible. Similarly, these difficulties prevent an experimental determination of either k_{30} or $\Delta H_f^\circ{}_{298}(C_6H_5O^\bullet)$.

The rate of CO formation predicted by the model is not particularly sensitive to the choice of k_{30}, as an increase here leads to a corresponding increase (through K_{30}) in k_{-30}. It is much more sensitive to the value of $\Delta H_f^\circ{}_{298}(C_6H_5O^\bullet)$. For example, increasing this value from 9.2 to 12.8 kcal·mol^{-1} leads to a similar curve, but it is now offset about 0.7 log units below the experimental points. In this respect, the present work supports the lower values for $\Delta H_f^\circ{}_{298}(C_6H_5O^\bullet)_g$. The model is also rather sensitive to ΔS_{30} and even small errors here could have significant effects; for example, increasing ΔS_{30} by 0.7 eu leads to almost perfect agreement between theory and experiment. The uncertainties in $S^\circ{}_{298}(C_6H_5O^\bullet)$ and C_p° terms are easily large enough to accommodate such changes and, overall, the agreement is remarkably good.

The orders of reaction for CO formation predicted by the model are shown in Figure 10 and are very close to zero. The extent and variation of this dependence is sensitive to both the choice of k_{30} and $\Delta H_f^\circ{}_{298}(C_6H_5O^\bullet)_g$; similar, or even better, agreement with experiment can be obtained with other values, but, in any case, Figure 10 demonstrates that the dependence can be very slight.

That there is no evidence for even a slight dependence at any temperature may in part be due to an oversimplified model. For example, other radicals formed during thermolysis can also lead to phenoxy radicals (32, exemplified for $^\bullet CH_3$), a reaction in competition with H abstraction from H_2, (33). Because of loss

$$^\bullet CH_3 + C_6H_5OH \rightarrow CH_4 + C_6H_5O^\bullet \qquad (32)$$

$$^\bullet CH_3 + H_2 \rightarrow CH_4 + H^\bullet \qquad (33)$$

of rotational entropy in the transition state, the A factor for reactions such as (32) will be ca. 2 log units lower than for the abstraction by $H^\bullet$, (30). [For example, the parameters for $CH_3^\bullet + CH_3OH \rightarrow CH_4 + CH_3O^\bullet$ are reported[35] as log k/M^{-1} s^{-1} = 7.9 − 9.0 kcal·mol^{-1}/2.3RT.] Because of this and the large excess of H_2, abstractions by $R^\bullet$ will not be the primary phenoxy radical forming reactions under our conditions; nonetheless, these reactions will occur. Further, as the H_2 concentration is decreased, the ratio $\sum[R^\bullet]/[H^\bullet]$ will increase, and such reactions will become relatively more important.

Re-formation of phenol from phenoxy radical may also be more complex. Because R_{-30} is not particularly high, disproportionation reactions of phenoxy with various organic radicals, $RH^\bullet$ (35, exemplified for cyclopentenyl, **4**), could be important under some circumstances.

$H^\bullet$ + CP $\rightleftharpoons$  (34)

4

$$\mathbf{4} + C_6H_5O^\bullet \rightleftharpoons C_6H_5OH + CP \qquad (35)$$

With an overall rate of disproportionation, $R_{dis} = k_{dis}[\Sigma RH^\bullet]$, and taking $k_{dis} \approx 10^{9.3}$ M^{-1} s^{-1}, we calculate that, for H_2 = 1 atm, $R_{-30} = R_{dis}$ if $[\Sigma RH^\bullet] = 10^{-7.0}$ M. Only stabilized radicals could begin to approach these concentrations, but precise estimates are difficult because of uncertainties in the heats of formation of such compounds. The generally higher C–H bond strengths proposed by Tsang[37] and others would indicate that these reactions are unimportant, while the older recommendations of McMillen and Golden[38] suggest that they could play a minor role ($R_{dis} \leq 0.10R_{-30}$) under some of our experimental conditions. Note, however, that these reactions will become increasingly important under more pyrolytic conditions and higher concentrations of organic compounds. Thus, although reactions of the type (32–35) appear to be relatively unimportant under our conditions, their presence may tend to further level out the dependence of CO formation on the H_2 concentration.

In fact, Figure 6 shows that rates of CO formation in phenol pyrolysis systems are remarkably close to those found in hydrogenolysis. We have derived here that this cannot be due to a molecular reaction, as has been previously supposed,[6] and is almost certainly due to phenoxy radical. In retrospect, the importance of phenoxy radical in phenol pyrolysis is not surprising. High radical concentrations are expected under pyrolytic conditions and the relatively weak O–H bond of phenol will be vulnerable to attack by a wide variety of species. This suggestion is fully compatible with the results of the earlier studies; Cypres and Bettens[6,7] reported H_2 as a major product in phenol pyrolysis, which suggests that H atoms play a role even when H_2 is not added per se. Further, they have invoked the presence of a large number of other radicals in order to explain the formation of many of their products.

Surface Effects and the Hydrogen Atom Concentration. It is well-known that quartz surfaces adsorb H atoms and catalyze the recombination of $H^\bullet$. Numerous studies[39-41] of these reactions have been made, mostly at temperatures <500 K. Such processes can be described by reactions 36–38, where W–H represents a

$$H^\bullet + W_0 \rightleftharpoons W\text{–}H \qquad (36)$$

$$H^\bullet + W\text{–}H \rightleftharpoons W_0 + H_2 \quad \text{Rideal mechanism} \quad (37)$$

$$2W\text{–}H \rightleftharpoons 2W_0 + H_2 \quad \text{Hinshelwood mechanism} \quad (38)$$

surface-adsorbed H atom and W_0 an empty adsorption site. At present the extent of each recombination reaction is uncertain,

---

(37) Tsang, W. *J. Am. Chem. Soc.* **1985**, *107*, 2872.

(38) McMillen, D. F.; Golden, D. M. *Annu. Rev. Phys. Chem.* **1982**, *33*, 493.

(39) Wood, B. J.; Wise, H. *J. Phys. Chem.* **1962**, *66*, 1049.

(40) (a) Lynch, K. P.; Michael, J. V. *Int. J. Chem. Kinet.* **1978**, *10*, 233. (b) Ahumada, J. J.; Michael, J. V. *J. Phys. Chem.* **1974**, *78*, 465 and references cited therein.

(41) Gelb, A.; Kim, S. K. *J. Chem. Phys.* **1971**, *55*, 4935 and references cited therein.

though some evidence[41] suggests the Rideal mechanism is dominant. The precise rate of surface recombination will depend on the pressure, temperature, and the geometry and S/V ratio of the reactor. Nonetheless, certain general observations can be made. At sufficiently low temperatures, equilibrium 36 lies far to the right and essentially all adsorption sites are occupied; recombination will then be first order in [H$^\bullet$]. At temperatures >500 K,[39] the number of occupied sites becomes proportional to [H$^\bullet$], and recombination is second order in [H$^\bullet$]. Finally, at still higher temperatures (>1100 K),[39] equilibrium 36 lies far to the left and the recombination rate approaches zero.

The sum of these processes has been approximated by Sepehrad et al.[42] and others as a single reaction

$$H^\bullet \rightarrow {}^1\!/_2H_2 \qquad (39)$$

and first-order rate constants have been reported. Cao and Back[15] have attempted to estimate k_{-39} from K_{39} (equal to $K_{19}{}^{1/2}$) and k_{39} reported at 775 K by Sepehrad et al.[42] The most obvious problem with this procedure is that the rate in the forward direction is not correctly described by a first-order rate constant. A general discussion on the dangers of estimating reverse rates of overall reactions via the equilibrium constant may be found elsewhere.[43]

Thus, while the basic premise of Cao and Back seems correct, namely that surface reactions can contribute to the equilibration of the hydrogen atom concentration, we think it remains difficult to accurately estimate the rates of these processes.

With regard to the effect of treatment of the reactor with NaOH, Kanan et al. have used this procedure in the pyrolysis of propane[11a] and ethane[11b] to enhance the rate of chain terminations occurring on the surface. They have attributed this to (39) and reported a value of $k_{39}/\text{s}^{-1} \geq 10^{4.2}$, at least 3 orders of magnitude greater than that reported in untreated reactors. If their description is correct, this would lead to faster equilibration of the H atom concentration. In fact, the chain termination step is not at all well established. Pacey and Wimalasena[44] examined the pyrolysis of ethane in reactors with different surfaces with the aim of determining the chain termination step. They reported that it was $C_2H_5^\bullet \rightarrow$ wall in all cases except for NaOH surfaces, where the data unfortunately did not permit a firm conclusion to be drawn.

In the present system, because H-atom addition reactions have high rate constants (typically 10^9–10^{10} M^{-1} s^{-1}), reactions 40 and 41 could lead to rapid removal of H atoms from the system. Since

$$H^\bullet + R \rightleftharpoons RH^\bullet \qquad (40)$$

$$RH^\bullet \rightarrow \text{wall} \qquad (41)$$

gas-phase dissociation of H_2 is slow, this could reduce the concentration of H$^\bullet$ below its equilibrium value, thus accounting for the much lower rates observed in the NaOH-treated reactor. At present, we feel this is the most likely explanation.

The evidence for equilibration in clean quartz reactors under our conditions is as follows: (1) the apparent reasonableness of the parameters for (22), (2) the first-order behavior of the reaction with respect to phenol, (3) the lack of an effect caused by a change in the S/V ratio, (4) excellent agreement between experimental and modeled CO formation rates based on equilibrium H$^\bullet$, and (5) based on the equilibrium assumption, we find at 1000 K an overall rate of $10^{9.65}$ M^{-1} s^{-1} for the process $H^\bullet + C_6D_6 \rightarrow C_6D_5H + D^\bullet$. The extrapolated parameters of Nicovich and Ravishankara[20] entail an addition rate constant of $10^{9.71}$ M^{-1} s^{-1}, which further suggests that the rate of addition is close to the rate of exchange, due to scrambling of hydrogen atoms in the cyclohexadienyl adduct. Similarly Sauer and Mani's results on $H^\bullet + C_6H_6$[45] lead to k(addition) 1000 K = $10^{9.83}$ M^{-1} s^{-1} (Nicovich et al. observed no isotope effect for $H^\bullet + C_6H_6/C_6D_6$, so these parameters should be comparable). Although exact comparison with these studies is not possible, as we have measured a slightly different process, the overall agreement is obviously good.

The evidence against is the lower rate of phenol conversion obtained in a reactor which possibly enhances the equilibration rate of (19). This is, however, based on the highly uncertain nature of the chain termination step(s) in NaOH treated reactors, as well as the assumption that surface reactions are a major source of H atoms in our system. We therefore feel that the majority of the evidence suggests that the hydrogen atom concentration is at equilibrium in clean quartz reactors under the conditions used here.

In sum, thermal hydrogenolysis of phenol at 1050 ± 125 K leads to two primary products, benzene and CO. Their sum is close to 100% of the converted phenol, whereas the measured C_6H_6/CO ratio varies from ca. 2.0 at 950 K, via unity at 1060 K, to 0.6 at 1150 K. Phenol conversion is nearly complete at he latter temperature, and the yield of CO is 64%. Benzene arises via ipso substitution of OH by H atoms (22), which appear to be present in thermodynamic equilibrium with H_2. Carbon monoxide stems from phenoxy radicals (29) rather than directly from phenol, or its keto form.

After submitting our paper, we learned about the results of the shock-wave study by He, Mallard, and Tsang.[49] They generated H atoms by decomposition of *tert*-butyl radicals (in turn formed from hexamethylethane) which could react with phenol, also in competition with methane. Using known rate parameters for the $CH_4 + H^\bullet$ reactions, measured benzene yields resulted in log k_{22} = 10.34 − 7920/2.3RT (1000–1150 K). Although these parameters differ by 0.5 log A and 2.5 kcal·mol^{-1} from ours, log k_{22} values are equal well within 0.1 unit over this temperature range. Considering the widely different experimental approaches this is a very satisfying result.

He et al. did not measure CO formation but have derived this product channel by the difference between benzene formed and phenol disappeared (in fact, H generated). On this basis, they report log k_{30} = 11.06 − 12390/2.3RT. As a consequence, the (calculated) C_6H_6/CO product ratio should be 1.8 at 1000 K, and 1.35 at 1150 K (or a selectivity to CO of 42.5% in the latter case). This is at variance with our measured values, with CO predominating above 1100 K. Note that in both systems the chemistry around $C_6H_5O^\bullet$ is rather complex, and He et al. had to take the reaction $C_6H_5O^\bullet + H^\bullet \rightarrow C_6H_5OH$ (−28) into account. As to the rate parameters for reaction 30, there is a substantial discrepancy between our "best estimate" and He's values; they may well deviate from the truth, and call for more direct experimental verification.

Acknowledgment. Financial support from the Dutch Ministry of Housing, Physical Planning, and Environmental Affairs, and by Akzo Zout Chemie, Hengelo, The Netherlands, is gratefully acknowledged.

Appendix

Heat of Formation of Phenoxy Radical. Values of 9–12.8 kcal·mol^{-1} for $\Delta H_f{}^\circ{}_{298}(C_6H_5O^\bullet)_g$ have been proposed.[29,31] The commonly accepted value is 11.4 kcal·mol^{-1} [38] and is based on Colussi et al.'s[29] VLPP measurement of ΔH for $C_6H_5OR \rightarrow C_6H_5O^\bullet + R^\bullet$, with R = C_2H_5 and C_3H_5 (allyl). If, however, for the R = C_2H_5 case, the revised value $\Delta H_f{}^\circ{}_{298}(C_2H_5^\bullet)_g$ = 28.36 ± 0.2 kcal·mol^{-1} [46] is used, the same data lead to $\Delta H_f{}^\circ{}_{298}(C_6H_5O^\bullet)_g$ = 9.4 kcal·mol^{-1}. The situation with R = C_3H_5 is less clear: the heat of formation of allyl radical is still uncertain, with recently suggested values[31,38,47] in the range of 39.1–43.7 kcal·mol^{-1}; in conjunction with the data of Colussi et al., these lead to $\Delta H_f{}^\circ{}_{298}(C_6H_5O^\bullet)_g$ = 7.4–11.1 kcal·mol^{-1}. Mulder et al.[48] have

---

(42) Sepehrad, A.; Marshall, R. M.; Purnell, J. H. *J. Chem. Soc., Faraday Trans. 1* **1979**, *75*, 835.

(43) Laidler, K. *Chemical Kinetics*, 3rd ed.; Harper and Row: New York, 1987.

(44) Pacey, P. D.; Wimalasena, J. H. *Can. J. Chem.* **1983**, *61*, 1086.

(45) Sauer, Jr., C. M.; Mani, I. *J. Phys. Chem.* **1970**, *74*, 59.

(46) Brouard, M.; Lightfoot, P. D.; Pilling, M. J. *J. Phys. Chem.* **1986**, *90*, 445.

(47) Tsang, W. *J. Phys. Chem.* **1984**, *88*, 2812.

(48) Mulder, P.; Saastad, O. W.; Griller, D. *J. Am. Chem. Soc.* **1988**, *110*, 4090.

recently used a photoacoustic technique to measure ΔH in solution for $t\text{-}C_4H_9O^\bullet + C_6H_5OH \rightarrow t\text{-}C_4H_9OH + C_6H_5O^\bullet$; from their data, they have determined $\Delta H_f^\circ{}_{298}(C_6H_5O^\bullet)_g = 9.0 \pm 1$ kcal·mol^{-1}. In view of the uncertainty in $\Delta H_f^\circ{}_{298}(\text{allyl})_g$, we prefer to average the Mulder et al. value with that obtained from Colussi et al.'s data on C_6H_5OEt decomposition. This gives $\Delta H_f^\circ{}_{298}(C_6H_5O^\bullet)_g = 9.2$ kcal·mol^{-1} and, as we have outlined, the present work supports this lower value.

Registry No. C_6H_5OH, 108-95-2.

---

(49) He, Y. Z.; Mallard, W. G.; Tsang, W. *J. Phys. Chem.* **1988**, *92*, 2196.

Sodium Atom Reactions with the Bromochloromethanes: Branching Ratios and Relative Reaction Rates

J. T. Jayne and P. Davidovits*

Department of Chemistry, Boston College, Chestnut Hill, Massachusetts 02167 *(Received: May 12, 1988; In Final Form: November 17, 1988)*

Branching ratios into bromide and chloride products have been measured for the reaction of atomic sodium with $BrCCl_3$, $BrCHCl_2$, and $BrCH_2Cl$. The bromide to chloride product ratios are 0.55, 1.83, and 4.00, respectively. The experiments were performed in a linear flow tube apparatus at 340 K. Sodium halide reaction products were collected along the flow tube and analyzed titrimetrically. In a separate set of experiments the relative reactivities of the bromine and chlorine sites in each of the molecules as well as in CH_3Br and $CHCl_3$ were determined by normalization to the reactivity of CCl_4. Semiempirical MNDO computer calculations were performed on the halomethane reactants to explore possible systematic correlations with the experimental data.

Introduction

The reactions of halomethanes with alkali-metal atoms have been studied extensively.[1-20] These molecules are well suited for systematic studies such as, for example, the testing of the effect of electronegative substituents on reactivity. Most of the studies done in the past were designed to characterize the sequence of reactivities for a set of molecules. For example, Heller and Polanyi[1] drew attention to the fact that the marked progressive increase in reactivity on passing along the series CH_3Cl to CCl_4 runs parallel to a decreasing force constant for the C–Cl bond. Increased reactivity is also observed by substitution of an existing halogen by a less electronegative halogen.[2] This too corresponds to a decreased force constant for the C–X bond. The results of some of these experiments lead to the formulation of the Bell–Evans–Polanyi principle relating activation energies to heats of reactions which has been used for the prediction of reaction rates.[21]

In most of the above studies total reaction rates have been measured. Branching ratios into product halides have been obtained in only one study for the reaction of sodium with the chlorofluoromethanes.[3] In this paper we present results of experiments in which branching ratios into bromide and chloride products were measured for the reaction of sodium atoms with the bromochloromethanes $BrCH_2Cl$, $BrCHCl_2$, and $BrCCl_3$. In a separate set of experiments the relative reactivities of the bromine and chlorine sites in each of the molecules as well as in CH_3Br and $CHCl_3$ were determined by normalization to the reactivity of CCl_4.

The reactions of sodium with these molecules to form a bromide or chloride product are in all cases exoergic. The exoergicities are in the range of 1.4 to 1.7 eV depending on the specific reaction, being highest for the formation of NaBr from $BrCCl_3$ and lowest in the formation of NaCl from $CHCl_3$.[22]

Experimental Procedure and Results

The experimental apparatus is shown in Figure 1. Sodium atoms are produced in a resistively heated oven and are entrained by a nitrogen carrier gas flow. The halomethane molecules are introduced into the flow through a perforated loop. The reaction products are formed, deposited along the flow tube, and collected for analysis.

The resistively heated oven consists of a cylindrical stainless steel crucible 3-in. in length with 1-in. o.d. and $^1/_8$-in. wall. The crucible was modeled after a design by Gole et al.[23] A section

---

(1) Heller, W.; Polanyi, M. *Trans. Faraday Soc.* **1936**, *32*, 633.
(2) Haresnape, J. N.; Stevels, J. M.; Warhurst, E. *Trans. Faraday Soc.* **1940**, *36*, 465.
(3) Kaufman, E. D.; Reed, J. F. *J. Phys. Chem.* **1963**, *67*, 896.
(4) Heller, W. *Trans. Faraday Soc.* **1937**, *33*, 1556.
(5) *CRC Handbook of Bimolecular and Termolecular Gas Reactions*; Kerr, J. A., Ed.; Chemical Rubber Co.: Boca Raton, FL, 1981.
(6) Lin, K. K.; Balling, L. C.; Wright, J. J. *Chem. Phys. Lett.* **1987**, *133*, 246.
(7) Frommer, L.; Polanyi, M. *Trans. Faraday Soc.* **1934**, *30*, 519.
(8) Fairbrother, F.; Warhurst, E. *Trans. Faraday Soc.* **1935**, *31*, 987.
(9) Warhurst, E. *Trans. Faraday Soc.* **1939**, *35*, 674.
(10) von Hartel, H.; Polanyi, M. *Z. Phys. Chem., Abt. B* **1930**, *11*, 97.
(11) von Hartel, H.; Meer, N.; Polanyi, M. *Z. Phys. Chem., Abt. B* **1932**, *19*, 139.
(12) Husain, D.; Marshall, P. *Int. J. Chem. Kinet.* **1986**, *18*, 83.
(13) Husain, D.; Marshall, P. *J. Chem. Soc., Faraday Trans. 2* **1985**, *81*, 613.
(14) Gowenlock, B. G.; Thomas, K. E. *J. Chem. Soc.* **1965**, 5068.
(15) Reed, J. F.; Rabinovitch, B. S. *J. Chem. Phys.* **1957**, *27*, 988.
(16) Husain, D.; Lee, Y. H. *Int. J. Chem. Kinet.* **1988**, *20*, 233.
(17) Warhurst, E. *Q. Rev. Chem. Soc.* **1951**, *5*, 44.
(18) Trotman-Dickenson, A. F. *Gas Kinetics*; Butterworths: London, 1955; p 219.
(19) Polanyi, M. *Atomic Reactions*; Williams and Norgate: London, 1932.
(20) Hodgins, J. W.; Haines, R. L. *Can. J. Chem.* **1952**, *30*, 473.
(21) Dewar, M. J. S.; Dougherty, R. C. *The PMO Theory of Organic Chemistry*; Plenum Publishing: New York, 1975.
(22) Vedenyev, V I.; Gurvich, L. V.; Kondratyev, V. W.; Medvedev, V. A.; Frankevich, Ye. L. *Bond Energies, Ionization Potentials, and Electron Affinities*; St. Martin's: New York, 1966.
(23) Preuss, D. R.; Pace, S. A.; Gole, J. L. *J. Chem. Phys.* **1979**, *71*, 3553.

0022-3654/89/2093-3574$01.50/0